Low-Frequency Equatorial Waves in Vertically Sheared Zonal Flow. Part I: Stable Waves

BIN WANG AND XIAOSU XIE

Department of Meteorology, University of Hawaii, Honolulu, Hawaii

(Manuscript received 28 December 1994, in final form 10 August 1995)

ABSTRACT

The mechanism by which a vertically sheared zonal flow affects large-scale, low-frequency equatorial waves is investigated with two-level equatorial β-plane and spherical coordinates models.

Vertical shears couple baroclinic and barotropic components of equatorial wave motion, affecting significantly the Rossby wave and westward propagating Yanai wave but not the Kelvin wave. This difference results from the fact that the barotropic component is a modified Rossby mode and can be resonantly excited only by westward propagating internal waves. The barotropic components emanate poleward into the extratropics with a pronounced amplitude, while the baroclinic components remain equatorially trapped. A westerly vertical shear favors the trapping of Rossby and Yanai waves in the upper troposphere, whereas an easterly shear tends to confine them in the lower troposphere. As such, their westward propagation is slowed down by both westerly and easterly shears. When the strength of the vertical shear varies with latitude, both the vertical modes are locally enhanced in the latitudes of strong shear.

The theory suggests that the vertical shear plays an essential role in emanation of heating-induced internal equatorial Rossby waves into the extratropics with a transformed barotropic structure. It may also be partially responsible for trapping perturbation kinetic energy in the upper-troposphere westerly duct and the lower-troposphere monsoon trough.

1. Introduction

Low-frequency tropical atmospheric waves induced by condensational heating usually penetrate vertically the entire troposphere where the background flow often has prominent vertical and meridional shears. The latter can potentially alter wave structure, propagation, and development. Study of the influences of mean flows on equatorial waves has been one of the fundamental problems in the tropical dynamics.

The earliest studies of mean flow effects on waves were stimulated by a need to explain the stratospheric quasi-biennial oscillation of zonal wind. The focus was on the interaction of *vertically propagating* internal waves with the mean flow. Lindzen (1970) demonstrated that both the equatorial Kelvin and Yanai (Yanai and Mauryama 1966) waves propagating in a vertically sheared zonal flow are absorbed shortly before reaching the critical levels where their frequencies are Doppler shifted to zero. Holton (1970) found that when Kelvin waves pass through a westerly vertical shear without a critical layer both vertical and latitudinal scales decrease and upward momentum transport becomes concentrated toward the equator. Boyd (1978a) conducted a comprehensive analysis of the effects of meridional shear of a zonal flow on vertically propagating waves of small vertical wavelength. Analytical solutions were obtained using a one-dimensional model in latitude. These solutions were further applied to a realistic tropical atmosphere (Boyd 1978b). The Kelvin waves were found to be negligibly influenced by even the strongest shears, whereas a shear with an observed strength may strikingly change vertical wavelengths of synoptic-scale Rossby waves and Yanai wave.

Another impetus for the study of mean flow effects stems from a need to interpret the global atmospheric response to tropical heating. The observed teleconnection patterns (e.g., Wallace and Gutzler 1981; Horel and Wallace 1981) were suggested to result from transmission of tropical perturbations, in the form of a Rossby wave train, from tropical heat source into extratropics (Hoskins and Karoly 1981; Webster 1981). Webster (1972) showed that the response has a baroclinic structure in the vicinity of the heat source but becomes equivalent barotropic away from the forcing region. Without vertical variation of the mean state, however, the thermally forced barotropic mode has a rather small amplitude (Lim and Chang 1983). Kasahara and Silva Dias's (1986) numerical experiments manifested that the vertical shear of mean flows permits a coupling of external and internal modes so that a significant barotropic response is generated. Lim and Chang (1986) examined the impacts of vertical shear,

Corresponding author address: Dr. Bin Wang, Dept. of Meteorology, School of Ocean and Earth Science and Technology, University of Hawaii, 2525 Correa Rd., Honolulu, HI 96822.
E-mail: bwang@soest.hawaii.edu

differential damping, and planetary boundary layer on the characteristics of the atmospheric response to specified internal heating. All three factors were found to enable the transfer of energy from internal mode to external mode motion. Their analysis, however, was based on an f-plane model in which the motion is assumed to be meridionally invariant so that neither equatorial waves nor midlatitude Rossby waves exist. These simplifications preclude the model's applicability to tropical wave motions. It remains to be revealed why equatorial tropospheric waves that have a predominant baroclinic structure transform themselves into a barotropic structure when emanating toward midlatitudes.

There are other wave phenomena that involve effects of mean flows. The maximum perturbation kinetic energy in the equatorial upper troposphere tends to coincide with mean westerlies (Murakami and Unninayer 1977; Arkin and Webster 1985), whereas the convective maxima tend to concur with easterlies (Murakami and Wang 1993). This implies that the energy sources for the transient disturbances in the equatorial westerly duct are remote. Webster and Holton (1982) extended Charney's (1969) theory of equatorward propagation of extratropical rotational waves and suggested that equatorial westerlies may act as a duct for penetration of midlatitude rotational mode into the Tropics, causing regional maxima in perturbation kinetic energy. An alternative explanation proposed by Webster and Chang (1988) was that the longitudinal convergence of the equatorial zonal flow shrinks the zonal wavelength of the Rossby waves so that their phase speed and group velocity vanish locally, producing an energy convergence to the *east* of the equatorial westerlies (the wave energy accumulation is thus not *in phase* with westerly maximum). Hoskins and Jin (1991) showed that large-scale equatorial Rossby waves were weakly dispersive and tend to move with a Doppler-shifted phase speed that allows it to "accumulate" to the east of an equatorial maximum of 10 m s^{-1} or more. While the above investigations highlighted the influences of the Doppler-shift latitudinal shear and longitudinal stretch deformation of a basic flow, the possible impact of the vertical shear was ruled out. The present study will explore whether vertical variations of a basic flow contribute to concentration of wave kinetic energy in the region of an upper-tropospheric westerly duct.

The major purpose of the current study is to assess the impacts of a vertically sheared zonal flow on low-frequency, gravest-mode equatorial waves and to illuminate the mechanisms by which vertical shears change wave properties. The roles of a meridional shear in modification of wave structure and dispersivity are also reexamined because the formulation of the theoretical models and the results are somewhat inconsistent in the previous studies (e.g., Wilson and Mak 1984; Zhang and Webster 1989). The perception gained from the present analysis is expected to shed light on some intriguing features of the tropical general circulation, such as the emanation of internal waves from equatorial to extratropical regions and the perturbation energy accumulation in the upper-tropospheric westerly duct and the lower-tropospheric monsoon troughs.

Part I of the current paper concentrates on propagation characteristics of vertically standing equatorial waves in a symmetric and dynamically stable basic flow. Part II examines the case in which the basic equatorial flow itself is dynamically unstable and examines the impacts of vertical shear on the instability arising from the interaction of equatorial waves with condensational heating.

To focus on basic mechanisms by which a mean state affects gravest-mode equatorial waves, we adopt prototype two-level models on an equatorial β plane and in spherical coordinates. The two-level model is one of the most powerful tools for understanding the dynamics of vertically standing modes with a gravest vertical structure. Its relevance to tropical motion lies in the fact that large-scale tropical waves are generated and maintained by condensational heating that stimulates primarily the gravest tropospheric baroclinic mode. The equatorial β-plane model is an extension of Matsuno's (1966) model by including a vertically and meridionally varying zonal flow. Its simplicity permits intuitive physical interpretation of the results. To check the validity of the equatorial β-plane approximation, we performed parallel computations using a spherical coordinate model. We demonstrate the qualitative validity of the equatorial β-plane model in study of equatorial wave emanation and its limitations.

2. The model

Consider perturbation motions in a basic tropical zonal flow that is geostrophic and varies with latitude and height. Equations governing inviscid, hydrostatic, perturbation motions on an equatorial β plane and in pressure (p) coordinates are

$$\frac{\partial u}{\partial t} + \bar{u}\frac{\partial u}{\partial x} + v\frac{\partial \bar{u}}{\partial y} + \omega\frac{\partial \bar{u}}{\partial p} - \beta y v = -\frac{\partial \phi}{\partial x}, \quad (2.1a)$$

$$\frac{\partial v}{\partial t} + \bar{u}\frac{\partial v}{\partial x} + \beta y u = -\frac{\partial \phi}{\partial y}, \quad (2.1b)$$

$$\frac{\partial u}{\partial x} + \frac{\partial v}{\partial y} + \frac{\partial \omega}{\partial p} = 0, \quad (2.1c)$$

$$\frac{\partial}{\partial t}\left(\frac{\partial \phi}{\partial p}\right) + \bar{u}\frac{\partial}{\partial x}\left(\frac{\partial \phi}{\partial p}\right) - \beta y v\frac{\partial \bar{u}}{\partial p} + S\omega = -\frac{RQ'}{C_p p}, \quad (2.1d)$$

where u, v, ω, and ϕ represent perturbation zonal and meridional winds, vertical p velocity and geopotential height, respectively; S is the static stability parameter for the dry atmosphere; Q' is the perturbation heating

rate; and R and C_p are the gas constant and specific heat at constant pressure.

Adopting a two-level model and writing momentum and continuity equations (2.1a–c) at the middle levels of the upper and lower troposphere, p_1 and p_2, and the thermodynamic equation (2.1d) at the level $p_m = 0.5(p_1 + p_2)$ yield

$$\frac{\partial u_1}{\partial t} + \bar{u}_1 \frac{\partial u_1}{\partial x} + v_1 \frac{\partial \bar{u}_1}{\partial y} + \omega_1 \frac{\bar{u}_2 - \bar{u}_1}{\Delta p} - \beta y v_1 = -\frac{\partial \phi_1}{\partial x}, \quad (2.2a)$$

$$\frac{\partial v_1}{\partial t} + \bar{u}_1 \frac{\partial v_1}{\partial x} + \beta y u_1 = -\frac{\partial \phi_1}{\partial y}, \quad (2.2b)$$

$$\frac{\partial u_1}{\partial x} + \frac{\partial v_1}{\partial y} + \frac{\omega_m}{\Delta p} = 0, \quad (2.2c)$$

$$\frac{\partial u_2}{\partial t} + \bar{u}_2 \frac{\partial u_2}{\partial x} + v_2 \frac{\partial \bar{u}_2}{\partial y} + \omega_2 \frac{\bar{u}_2 - \bar{u}_1}{\Delta p} - \beta y v_2 = -\frac{\partial \phi_2}{\partial x}, \quad (2.2d)$$

$$\frac{\partial v_2}{\partial t} + \bar{u}_2 \frac{\partial v_2}{\partial x} + \beta y u_2 = -\frac{\partial \phi_2}{\partial y}, \quad (2.2e)$$

$$\frac{\partial u_2}{\partial x} + \frac{\partial v_2}{\partial y} - \frac{\omega_m}{\Delta p} = 0, \quad (2.2f)$$

$$\frac{\partial}{\partial t}(\phi_2 - \phi_1) + \bar{u}_m \frac{\partial}{\partial x}(\phi_2 - \phi_1) - \beta y v_m (\bar{u}_2 - \bar{u}_1) + \Delta p S_m \omega_m (1 - I) = 0, \quad (2.2g)$$

where subscripts 1, 2, and m denote levels p_1, p_2, and p_m, respectively, and Δp is one-half the pressure depth of the troposphere. In derivation of (2.2a–g), the vertical pressure velocity at the upper and lower boundaries were assumed to vanish, and the heating rate at level p_m was parameterized as

$$-\frac{RQ'_m}{C_p p_m} = I S_m \omega_m, \quad (2.3)$$

which describes a precipitational heating rate that acts to reduce static stability of the atmosphere from S_m to $(1 - I)S_m$. The present study is concerned with a stable stratification only, that is, the nondimensional heating coefficient $I < 1$. In this paper, we assume $I = 0$; that is, the wave motion is adiabatic. For convenience, all dependent variables are partitioned into a barotropic and a baroclinic component, namely,

$$A_+ = \frac{1}{2}(A_1 + A_2), \quad A_- = \frac{1}{2}(A_1 - A_2), \quad (2.4)$$

where A represents horizontal velocities or geopotential and A_+ and A_- are referred to as a barotropic and baroclinic mode, respectively. They describe, respectively, vertical mean wind and thermal wind motion. For the baroclinic mode, the geopotential thickness and thermal wind can also be interpreted as upper-tropospheric perturbation geopotential and wind; the corresponding lower-tropospheric geopotential and wind are precisely 180° out of phase with their corresponding upper-tropospheric counterparts.

The governing equations were then written in terms of two vertical (barotropic and baroclinic) modes and were nondimensionalized using the internal gravity wave speed $C_m = (0.5\Delta p^2 S_m)^{1/2}$ as a velocity scale, the Rossby radius of deformation $L = (C_m/\beta)^{1/2}$ as a horizontal length scale, L/C_m as a timescale, C_m^2 as a geopotential scale, and $2\Delta p(\beta C_m)^{1/2}$ as a vertical p-velocity scale. In the present study, we assume $C_m = 51$ m s^{-1}. The following nondimensional equations were finally obtained after eliminating ω_m:

$$\frac{Du_+}{Dt} - (y - \bar{u}_y)v_+ + \frac{\partial \phi_+}{\partial x} = -2U_T \frac{\partial u_-}{\partial x} - \frac{\partial (U_T v_-)}{\partial y}, \quad (2.5a)$$

$$\frac{Dv_+}{Dt} + y u_+ + \frac{\partial \phi_+}{\partial y} = -U_T \frac{\partial v_-}{\partial x}, \quad (2.5b)$$

$$\frac{\partial u_+}{\partial x} + \frac{\partial v_+}{\partial y} = 0, \quad (2.5c)$$

$$\frac{Du_-}{Dt} - (y - \bar{u}_y)v_- + \frac{\partial \phi_-}{\partial x} = -U_T \frac{\partial u_+}{\partial x} - v_+ \frac{\partial U_T}{\partial y}, \quad (2.5d)$$

$$\frac{Dv_-}{Dt} + y u_- + \frac{\partial \phi_-}{\partial y} = -U_T \frac{\partial v_+}{\partial x}, \quad (2.5e)$$

$$\frac{D\phi_-}{Dt} + \frac{\partial u_-}{\partial x} + \frac{\partial v_-}{\partial y} = y v_+ U_T, \quad (2.5f)$$

where

$$\frac{D}{Dt} \equiv \frac{\partial}{\partial t} + \bar{U}\frac{\partial}{\partial x},$$

$$\bar{U} = \frac{1}{2}(\bar{u}_1 + \bar{u}_2),$$

and

$$U_T = \frac{1}{2}(\bar{u}_1 - \bar{u}_2).$$

For the convenience of theoretical analysis, both the vertical mean and vertical shear are decomposed as sums of a constant and a y-dependent function. In a linear model, the effects of each component can be identified through choice of specific mean zonal flows. In the subsequent three sections, we will investigate three specific basic flows to elucidate how a pure meridional shear, a constant vertical shear, and a com-

bined vertical–meridional shear affect equatorial wave dynamics.

3. Change of meridional structure and dispersivity by meridional shears

Without vertical shears, the barotropic and baroclinic modes are decoupled. The barotropic mode evolves, without interaction with the baroclinic mode, in the form of a nondivergent Rossby wave in an effective β (i.e., $\beta - \bar{U}_{yy}$) plane, whose behavior is well known. The baroclinic mode, on the other hand, satisfies the following modified shallow water equations:

$$\frac{Du_-}{Dt} - (y - \bar{U}_y)v_- = -\frac{\partial \phi_-}{\partial x}, \quad (3.1a)$$

$$\frac{Dv_-}{Dt} + yu_- = -\frac{\partial \phi_-}{\partial y}, \quad (3.1b)$$

$$\frac{D\phi_-}{Dt} + \frac{\partial u_-}{\partial x} + \frac{\partial v_-}{\partial y} = 0. \quad (3.1c)$$

From the above equations, the meridional structure of a zonally propagating baroclinic mode

$$(u_-, v_-, \phi_-) = R_e(U, V, \Phi)e^{i(kx-\sigma t)} \quad (3.2)$$

is governed by a set of ordinary differential equations with variable coefficients. By eliminating U and Φ, one ends up with a single equation for V:

$$V_{yy} + \frac{1}{c'}\left[2\bar{U}_y - \frac{2\bar{U}_y}{1 - c'^2}\right]V_y + \left[-k^2(1 - c'^2) - \frac{1 - \bar{U}_{yy}}{c'} + \frac{2\bar{U}_y(y - \bar{U}_y)}{1 - c'^2} - y(y - \bar{U}_y)\right]V = 0, \quad (3.3)$$

where $c' = \sigma/k - \bar{U}$ is the Doppler-shifted phase speed.

At the meridional boundaries $y = y_b$ and $-y_b$, the perturbation meridional wind is required to vanish in consistency with the equatorial-trapped nature of the low meridional index modes. This is somewhat unrealistic. However, a parallel study with a spherical coordinate model (see the appendix) shows that when the half-width of the equatorial β-plane channel is about four times the Rossby radius of deformation the gravest meridional mode—Kelvin wave, Yanai wave, and $n = 1$ Rossby wave—are not appreciably affected by the finiteness of the boundaries, consistent with our previous experience (Wang and Rui 1990). Since the present study deals with the gravest equatorial waves, the proposed boundary conditions are adequate.

Equation (3.3), along with the meridional boundary conditions, consists of an eigenvalue problem whose solution can be obtained by a shooting method (Langer 1960) or matrix inversion. To check the validity of the numerical computation, we use both methods.

To simulate the observed meridional variation of the mean zonal wind (Fig. 1a), two idealized profiles are examined (Fig. 1b): one has easterlies near the equator that will be referred to as the equatorial easterly (EE) profile, and the other has westerlies near the equator (EW profile hereafter). These profiles are similar to those used by Zhang and Webster (1989).

The presence of meridionally sheared flow EE and EW makes the baroclinic Rossby mode ($n = 1$) more tightly trapped near the equator compared with that in a resting atmosphere (Fig. 2). The trapping is stronger in mean flow EE due to the larger meridional shear between $y = 2$ and $y = -2$. The direction of the mean flow does not affect the trapping. The tight equatorial

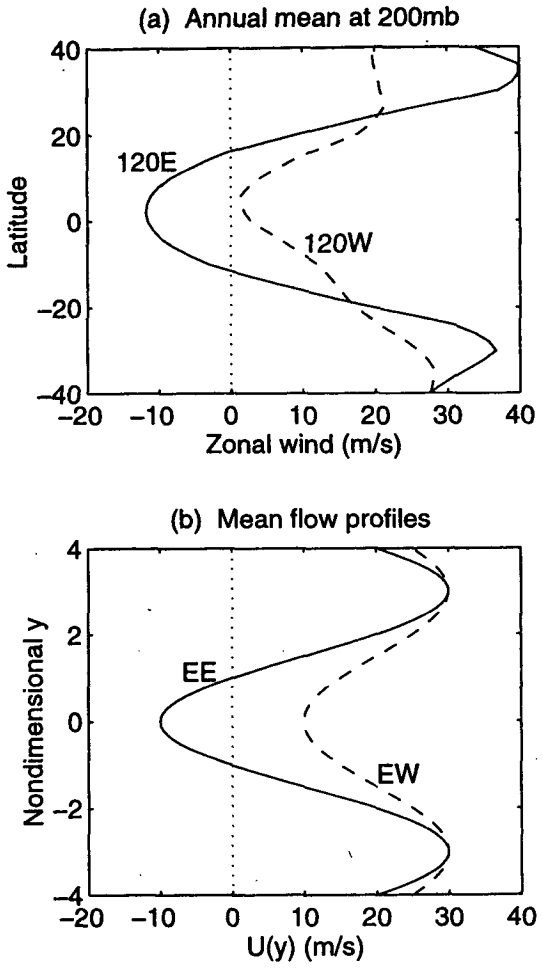

FIG. 1. (a) Annual-mean zonal flows at 200 hPa along 120°E (solid line) and 120°W (dashed line). The data are derived from the European Centre for Medium-Range Weather Forecasts global analyses for the period 1979–85. (b) Idealized mean zonal flows with meridional shear. The profile that includes equatorial easterlies is marked as EE (solid line), and the profile that has equatorial westerlies as EW (dashed line).

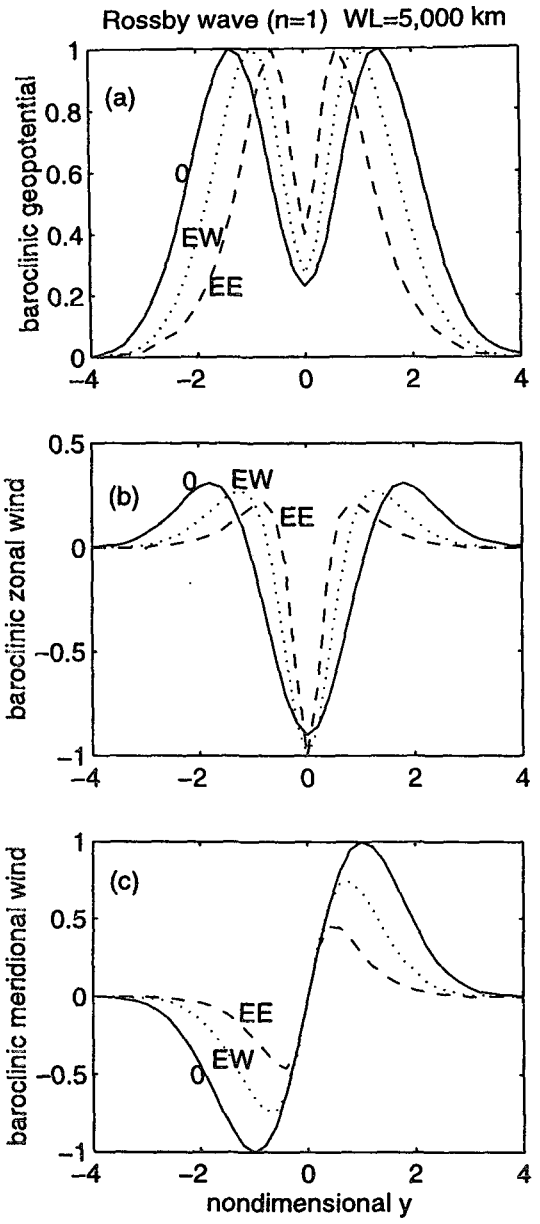

FIG. 2. Meridional structures of the Rossby wave (n = 1) with a wavelength of 5000 km, in the presence of meridionally sheared flow EE (dashed) and EW (dotted). Solid curves are for waves in a resting atmosphere. Curves in the three panels represent the amplitude of baroclinic (a) geopotential, (b) zonal wind, and (c) meridional wind. The profiles have been normalized by their corresponding maxima, but the zonal wind and the meridional wind have the same scale.

trapping gives rise to a large latitudinal gradient in geopotential thickness, and as a result, the zonal thermal wind is enhanced near the equator. The impact of meridional shear on equatorial trapping is more significant for short waves. For planetary-scale waves (zonal wave-number 1–4), modifications are negligible (figure not shown). The result here is consistent with that of Wilson and Mak (1984) but qualitatively different from that of Zhang and Webster (1989). The difference originates from the fact that the present model deals with the gravest baroclinic mode, which is presumably excited by internal heating, whereas Zhang and Webster's model describes an external mode for which their model's free-surface sloping associated with the mean zonal flow affected perturbation pressure, resulting in a weaker equatorial trapping and a dependence of trapping on the direction of mean flow.

In zonal flow EE, the westward phase speed of the baroclinic Rossby mode is faster than that without mean flows, whereas in zonal flow EW, the Rossby waves shorter than 10 000 km move eastward, while longer waves move westward (Fig. 3a). This is primarily due to the Doppler-shift effect of the basic flow. In the vicinity of the latitude where geopotential thickness reaches maximum amplitude, the basic zonal flow speed appears to be indicative of the strength of the Doppler-shift effects. From Fig. 2, for a Rossby wave with wavelength of 5000 km, the maximum amplitude of geopotential occurs at nondimensional y = 1 and 0.7 for EW and EE, respectively. The corresponding speeds at these latitudes are 13 m s^{-1} for EW and −3 m s^{-1} for EE (Fig. 1b). Obviously, these values are consistent with the magnitude of the Doppler-shifted speed for wavelength 5000 km (or k = 1.88) (Fig. 3a).

Because the degree of equatorial trapping increases with decreasing wavelength, one anticipates a more significant modification of phase speed for short waves by the Doppler-shifted effects in flow EE, as indicated in Fig. 3a. It follows that the wave dispersivity and group speed would be modified accordingly, as shown in Figs. 3b and 3c. The Doppler-shift effect has a major impact on the group velocity. These results are consistent with the conclusion derived from numerical modeling of the equatorial Rossby waves by Hoskins and Jin (1991).

The meridional shear also reinforces equatorial trapping for the baroclinic Kelvin mode (figure not shown). In addition, the degree of equatorial trapping increases with decreasing wavelength: short waves tend to be more tightly trapped to the equator than long waves. For the given two mean flow profiles, which have a minimum at the equator, the shorter waves are then expected to have a smaller eastward Doppler-shifted speed. This implies that shorter waves may have a slower eastward propagation speed. The computed Doppler-shifted phase speed for Kelvin waves in zonal flow EE and EW indeed shows an increase of phase speed with wavelength as we envisioned (figure not shown). Therefore, nondispersive equatorial Kelvin waves becomes weakly dispersive due to the modification of their meridional structure and nonuniform zonal advection by meridionally sheared flows.

In addition to the latitude-dependent zonal advection, the meridional shear affects wave properties by changing environmental vorticity gradient. The change

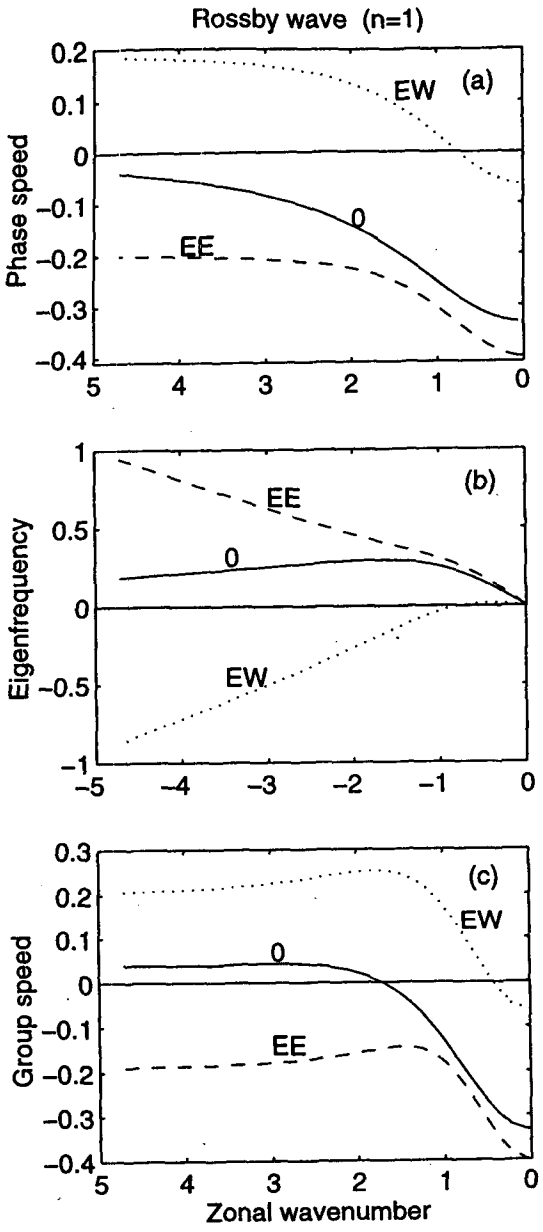

FIG. 3. Nondimensional (a) phase speed, (b) eigenfrequency, and (c) group speed of Rossby wave ($n = 1$) as a function of nondimensional zonal wavenumber k in meridionally sheared flow EE (dashed) and EW (dotted), compared to those in a resting atmosphere (solid). A wavelength of 9400 km corresponds to $k = 1.0$.

of the meridional wave structure depends on the sign and strength of the mean flow vorticity gradient. To demonstrate this dependence, additional computations were performed in which the zonal flows have signs opposite of those shown in Fig. 1 (referred to as case −EE and −EW, respectively). Of interest is that the Kelvin waves in a reversed zonal flow become less trapped (Fig. 4). This indicates that waves are more trapped to the equator if $U_{yy} > 0$ (case EE and EW), whereas they are less trapped when $U_{yy} < 0$ (case −EE and −EW) in the vicinity of the equator. The Coriolis force associated with zonal wind is no longer in perfect geostrophic balance with pressure gradient force due to modification of the β parameter by relative vorticity gradient ($-U_{yy}$) of the zonal flow. Consequently, the motion associated with Kelvin waves is no longer purely zonal: ageostrophic, meridional winds appear off the equator. The ratio of maximum meridional wind to maximum zonal wind is approximately one-half in the −EE case and one-sixth in the −EW case.

4. Excitation of barotropic mode and change of vertical structure by vertical shear

Upon knowing the effect of the pure meridional shear, we consider a basic zonal flow without meridional variation. Assume the vertical shear of the zonal flow is a constant. In this case, the barotropic and baroclinic modes are coupled by the vertical shear [Eqs. (2.5a–f)]. Since the barotropic mode is nondivergent [Eq. (2.5c)], it is convenient to introduce a barotropic streamfunction ψ, so that

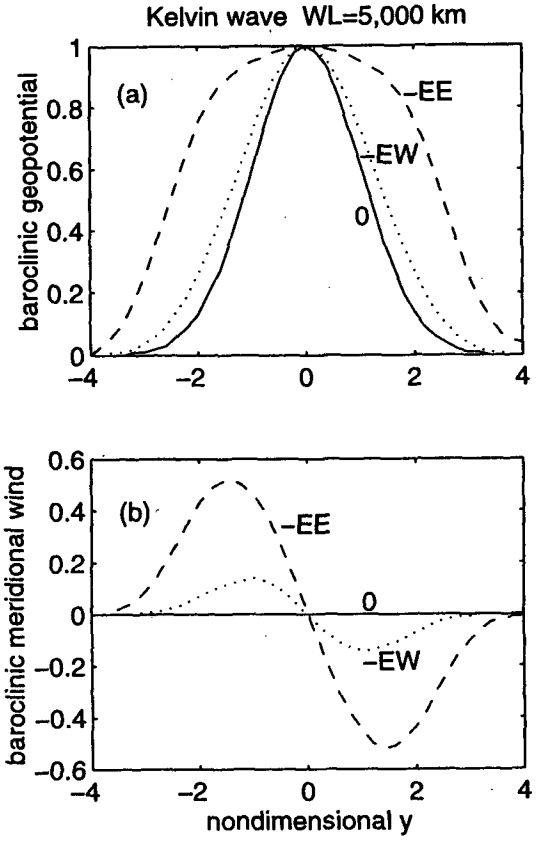

FIG. 4. (a) As in Fig. 2a and (b) as in Fig. 2c except for equatorial Kelvin waves in meridionally sheared flow −EE and −EW. The zonal flows in profiles −EE and −EW have opposite signs of profiles EE and EW (Fig. 1), respectively.

$$u_+ = -\frac{\partial \psi}{\partial y}, \quad v_+ = \frac{\partial \psi}{\partial x}. \tag{4.1}$$

The barotropic and baroclinic modes then satisfy

$$\frac{D}{Dt}\nabla^2\psi + \frac{\partial \psi}{\partial x} = U_T\left(\frac{\partial^2}{\partial y^2} - \frac{\partial^2}{\partial x^2}\right)v_- + 2U_T\frac{\partial^2 u_-}{\partial x \partial y}, \tag{4.2a}$$

$$\frac{Du_-}{Dt} - yv_- + \frac{\partial \phi_-}{\partial x} = -U_T\frac{\partial u_+}{\partial x}, \tag{4.2b}$$

$$\frac{Dv_-}{Dt} + yu_- + \frac{\partial \phi_-}{\partial y} = -U_T\frac{\partial v_+}{\partial x}, \tag{4.2c}$$

$$\frac{D\phi_-}{Dt} + \frac{\partial u_-}{\partial x} + \frac{\partial v_-}{\partial y} = yv_+U_T. \tag{4.2d}$$

Wave solutions of the form

$$(u_-, v_-, \phi_-, \psi) = R_e(U, V, \Phi, \Psi)e^{i(kx-\sigma t)} \tag{4.3}$$

satisfy a set of ordinary differential equations for the meridional structure functions, which can be derived by substituting (4.3) into (4.2). Further eliminating Φ and U from the resulting equations yields

$$\Psi_{yy}\left(1 + \frac{2U_T^2}{1-c'^2}\right) - \Psi_y\frac{2yU_T^2}{c'(1-c'^2)} - \left[k^2 - \frac{1}{c'} + \frac{2U_T^2}{c'(1-c'^2)}\right]\Psi = \frac{iU_T}{kc'}\left[\frac{1+c'^2}{1-c'^2}V_{yy} + \frac{2c'y}{1-c'^2}V_y - \left(k^2 - \frac{2c'}{1-c'^2}\right)V\right], \tag{4.4a}$$

$$V_{yy} - \left[y^2 + k^2(1-c'^2) - \frac{1}{c'}\right]V = -\frac{ikU_T}{c'}[\Psi_{yy} - 2yc'\Psi_y - (k^2(1-c'^2) + c' - y^2)\Psi], \tag{4.4b}$$

where $c' = \bar{U} - c$.

The meridional boundaries were located at $y = 4$ and -4 (about 60° latitude). The boundary conditions and the numerical methods for solving (4.4a) and (4.4b) are the same as those used in the meridional shear case. The vanishing of the barotropic meridional wind implies a constant barotropic streamfunction along the meridional boundaries.

a. *Rossby wave and westward propagating Yanai wave*

The forcing terms on the rhs of Eq. (4.4a) and (4.4b) indicate an interaction between the baroclinic and barotropic modes in the presence of vertical shear. It is interesting to recognize that for a constant vertical shear one of the vertical modes may have a structure that is independent of the sign of vertical shear but the remaining vertical mode must then have a structure dependent on the sign of shear; that is, the structure in a westerly shear should be exactly 180° out of phase with that in an easterly shear. Either vertical mode can be the candidate independent of the sign of shear. For instance, if we assume $\tilde{\psi} = U_T\psi$, the baroclinic mode (V) would not depend on the sign of vertical shear, because $\tilde{\psi}$ is an even function of the shear. In this case, however, the barotropic mode (ψ) must reverse its sign when vertical shear does. Equally valid is a reversed argument. It is important to point out that no matter which mode is assumed to be independent of the sign of shear the two vertical modes are in phase in westerly shears, whereas they are 180° out of phase in easterly shears. Based on this fact, in the following analysis we presume that the baroclinic mode structure is invariant with regard to the sign of the vertical shear.

Figure 5 shows meridional structures of the baroclinic and barotropic modes in the presence of vertical shear for the Rossby wave of the gravest meridional mode. The structures of the baroclinic modes are identical in easterly and westerly shears with the same strength (Fig. 5a). A moderate vertical shear of $U_T = 5$ ms^{-1} or $U_T = -5$ ms^{-1} makes the baroclinic mode slightly less equatorially trapped, especially for the zonal and meridional winds at the latitudes about one Rossby radius of deformation away from the equator. The meridional structure of the barotropic mode in an easterly shear is 180° out of phase with that in a westerly shear (Fig. 5b). Unlike the equatorially trapped pattern of the baroclinic mode, the barotropic geopotential expands poleward with largest amplitudes located near $y = \pm 3$ (three times the Rossby radius of deformation). The zonal winds, in a geostrophic balance with meridional geopotential gradients, reach maximum around $y = +2$ and $y = -2$, as well as at the equator. The large meridional variation of the zonal wind implies a salient relative vorticity pattern associated with the barotropic mode. Because the barotropic mode is nondivergent, the meridional variation of the meridional wind ($\partial v/\partial y$) must be in quadrature with the longitudinal variation of the zonal wind ($\partial u/\partial x$). Therefore, the meridional winds maximize or minimize on the latitudes where zonal wind vanishes. On the other hand, the zonal wind reaches extrema at the latitudes where the meridional wind vanishes (Fig. 5b).

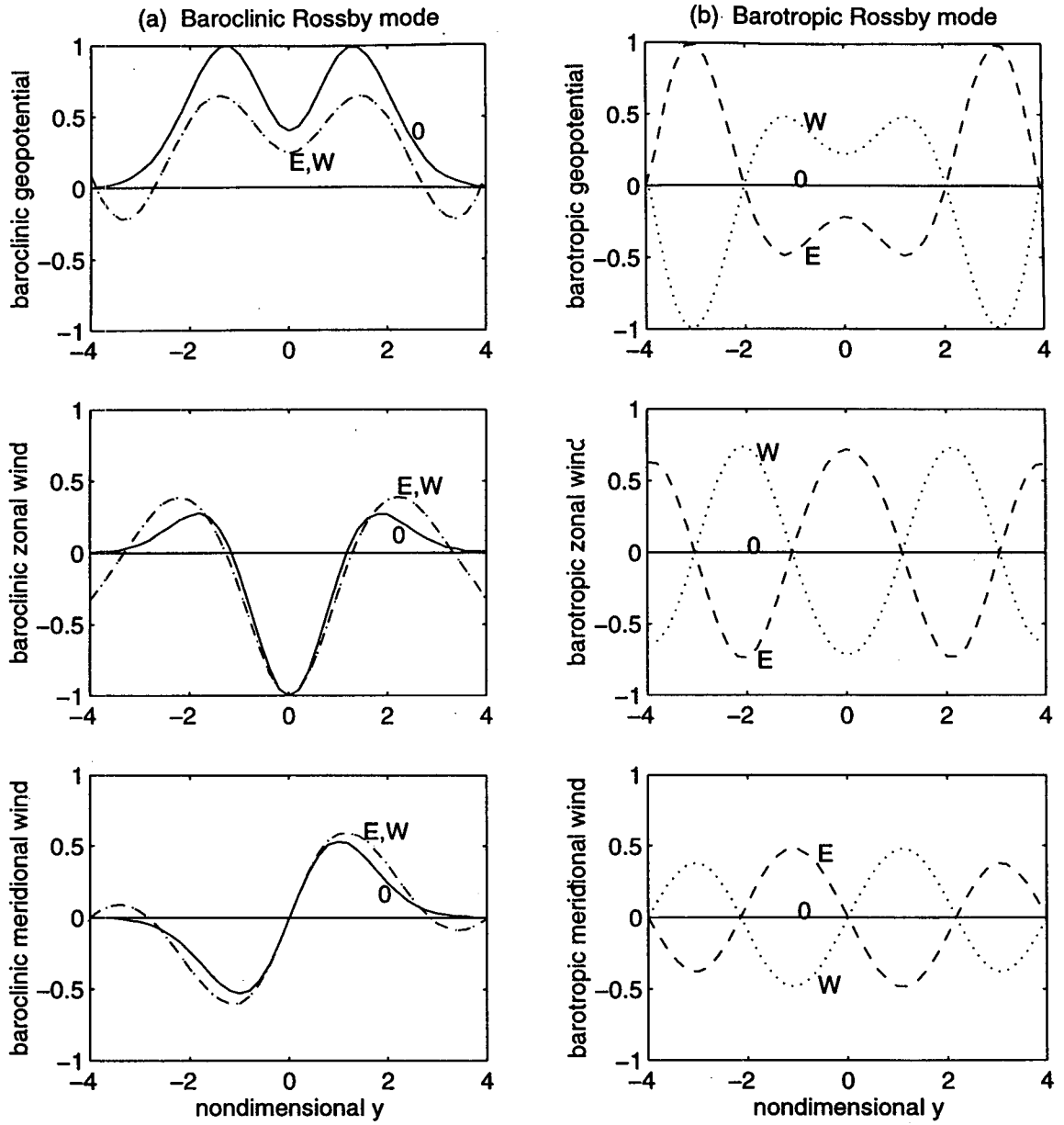

FIG. 5. Meridional structures of the (a) baroclinic and (b) barotropic Rossby mode ($n = 1$) calculated using an equatorial β-plane model. Solid, dashed, and dotted curves represent cases with vertical shears of $U_T = 0$, -5^{-1}, and 5 m s^{-1}. The upper, middle, and lower panels show the geopotential, zonal wind, and meridional wind.

Because the barotropic mode associated with Rossby waves is not equatorially trapped, it is necessary to check the applicability of the equatorial β-plane model. Figure 6 shows the meridional structures computed using spherical coordinates model. Comparison of Figs. 5 and 6 suggests that the β-plane results are qualitatively valid even for the untrapped barotropic mode. However, errors increase in high latitudes. The maximum geopotential perturbation of the barotropic mode is located at $y = 3$ (about 45°) in the β-plane model while it is shifted to about 57° in the spherical coordinate model (Figs. 5b and 6b). Due to the feedback of the barotropic mode, the baroclinic mode has significant amplitude around 60° (Fig. 6a).

The barotropic Rossby mode shown in Fig. 5b has an amplitude comparable to that of the baroclinic Rossby mode. Even in the vicinity of the equator, the geopotential and zonal wind of the two modes exhibit similar magnitudes. Ratios of the maximum amplitude of the barotropic versus baroclinic mode in geopoten-

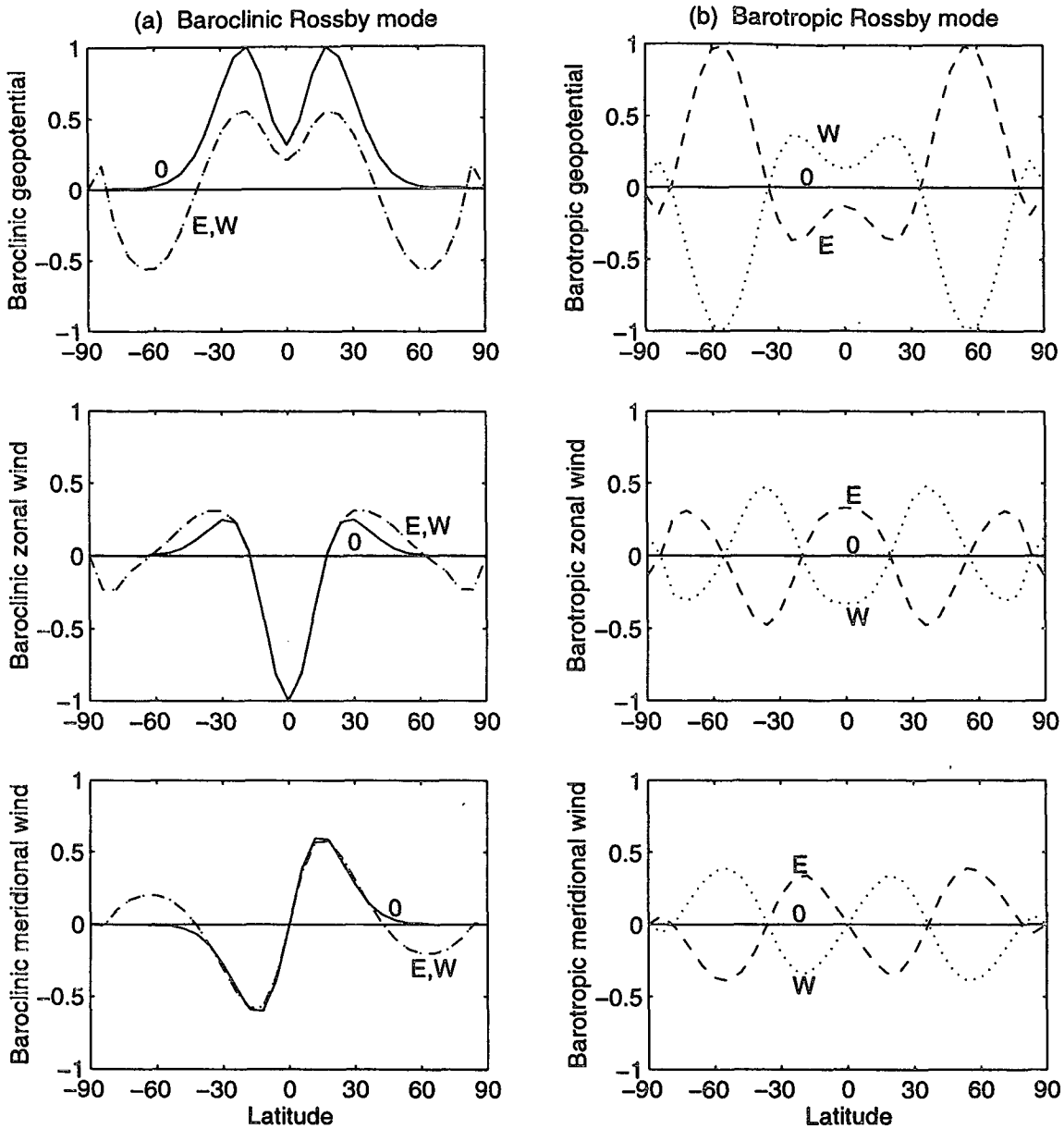

FIG. 6. As in Fig. 5 except computed from a spherical coordinates model.

tial (ϕ_+/ϕ_-), zonal (u_+/u_-), and meridional (v_+/v_-) winds all increase with increasing strength of the vertical shear, especially in the geopotential height field (Fig. 7). However, the ratios do not depend on the sign of vertical shear. The relative strength of the barotropic mode also tends to be stronger for shorter Rossby waves, as depicted by the downward tilt of the contours with decreasing wavelength in Fig. 7. The amplitude of the barotropic geopotential height exceeds its baroclinic counterpart when the magnitude of U_T exceeds about 3 m/s (Fig. 7a). In the real atmosphere, U_T is often larger than this value. One, therefore, anticipates a dominance of the barotropic response for the equatorial Rossby waves, especially for shorter waves and in the extratropics.

The comparative amplitudes of the two vertical modes have an important ramification for the Rossby wave's vertical structure. When the meridional structures of the two modes are nearly in phase, the perturbation attains a greater amplitude at the upper troposphere and a smaller amplitude at the lower troposphere because $A_1 = A_+ + A_-$ and $A_2 = A_+ - A_-$ [Eq. (2.4)]. This is the case in a westerly shear, where the meridional variations of geopotential (zonal and meridional

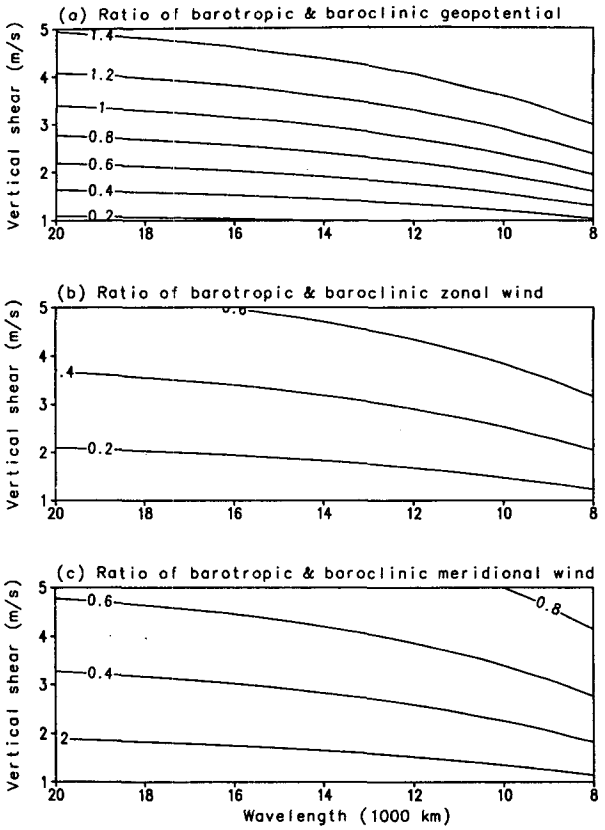

FIG. 7. Ratios of the maximum amplitudes of barotropic vs baroclinic mode for the $n = 1$ Rossby wave, as a function of wavelength and magnitude of vertical shear.

winds as well) for the two vertical modes tend to be in phase (Fig. 5). As a result, the perturbation is confined, to certain degrees, to the upper troposphere in the Tropics (Fig. 8a). On the other hand, in a zonal flow with an easterly vertical shear, the perturbation tends to be confined to the lower troposphere (Fig. 8b) because the baroclinic mode is nearly completely out of phase with the barotropic mode (Fig. 5). The asymmetry in the vertical structure results from the difference between the barotropic and baroclinic responses with regard to the sign of the vertical shear. Outside the Tropics ($|y| > 2$), the Rossby wave is barotropic due to the equatorial trapping of the baroclinic mode.

The westward propagation of the Rossby waves tends to be slowed down by the existing vertical shear, regardless of the sign of the shear (Fig. 9). Short waves are slightly more affected. This can be interpreted as follows. As shown earlier in Fig. 8, a westerly shear favors trapping perturbation in the upper troposphere. As such, the "steering" level for the perturbation is raised up above the middle level where the mean zonal flow vanishes; that is, the steering flow is eastward (Fig. 10a). The easterly shear, however, tends to restrain perturbation to the lower troposphere, and the corresponding steering level is thus lowered down below the middle level; thus, the steering flow is also eastward (Fig. 10b). In both easterly and westerly shears, the eastward steering of the mean flow would slow down the westward propagation of Rossby waves. The modification of phase speed depends on strengths of the vertical shear and wavelength. For a given shear, the structures of shorter waves are more significantly modified and so are their phase speeds.

For westward propagating Yanai waves, there is also a considerable response in barotropic geopotential, although responses in barotropic wind fields are relatively weak (figure not shown). Overall, the effects of vertical shear on the westward propagating Yanai wave is significant and analogous to those on Rossby waves except that the barotropic mode near the equator is dominated by the baroclinic counterpart.

b. Kelvin wave

In contrast to the significant effects on Rossby wave, vertical shears have little impact on equatorial Kelvin waves. The structure of the baroclinic mode is hardly affected by the vertical shear (figure not shown). A barotropic mode is excited, but its amplitude is at least one order of magnitude smaller than the corresponding baroclinic counterpart. Therefore, no appreciable change in the total perturbation field is found due to the presence of vertical shears.

Why are the Rossby waves strongly modified by vertical shears, while the Kelvin waves are little affected? This is due to the difference in excitation of the barotropic mode: the baroclinic Rossby mode is much more efficient in generating the barotropic mode than the baroclinic Kelvin mode. This difference may be explained as follows.

The barotropic mode is governed by nondimensional vorticity equation, Eq. (4.2a), which can be recast to

$$\underset{\text{(A)}}{\frac{D\zeta_+}{Dt}} = \underset{\text{(B)}}{-v_+} + \underset{\text{(C)}\quad\text{(D)}}{U_T\left(\frac{\partial D_-}{\partial y} - \frac{\partial \zeta_-}{\partial x}\right)}. \tag{4.5}$$

Term (A) includes rate of local change and mean flow advection of barotropic vorticity. When $\bar{U} = 0$ (as the cases here), the term (A) represents the rate of local change of barotropic vorticity. Term (B) is the meridional advection of the planetary vorticity by barotropic motion. Terms (C) and (D) denote a forcing induced by the combined effect of the baroclinic motion and vertical shear. This forcing will be referred to as baroclinic forcing that is proportional to the magnitude of the vertical shear. It is associated with the meridional gradient of baroclinic divergence and longitudinal gradient of baroclinic vorticity. Equation (4.5) indicates that the barotropic mode is a nondivergent vorticity wave that is maintained by barotropic planetary vorticity advection (the β effect) and the baroclinic forcing.

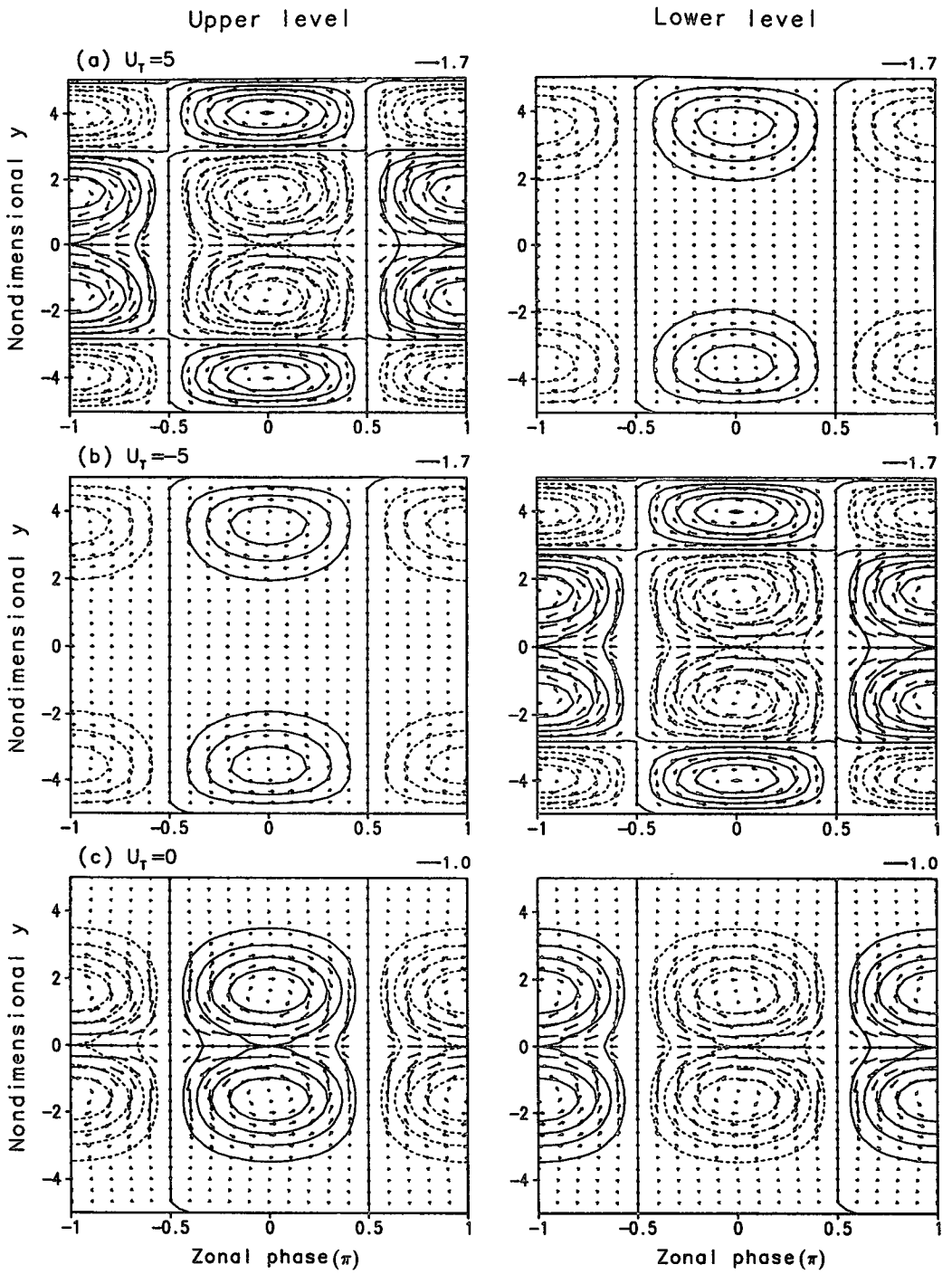

FIG. 8. Horizontal structures of the $n = 1$ Rossby wave with a wavelength of 10 000 km. Geopotential and flow patterns in the upper and lower troposphere are displayed for (a) $U_T = 5$ m s^{-1}, (b) $U_T = -5$ m s^{-1}, and (c) $\bar{U} = 0$.

For a Rossby wave, the baroclinic divergence is at least an order of magnitude smaller than the baroclinic vorticity. The baroclinic forcing owes its origin primarily to the longitudinal stretch of baroclinic vorticity. On the other hand, for a Kelvin wave, the longitudinal variation of baroclinic vorticity and the meridional variation of baroclinic divergence have comparable amplitudes, thus, both have a competitive contribution to baroclinic forcing (figure not shown). Although the strength of the forcing varies with wavelength, numer-

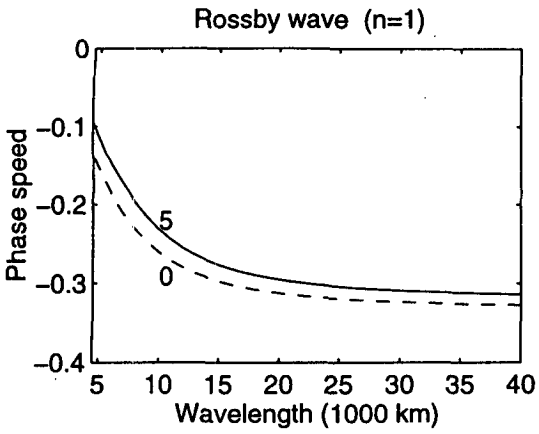

FIG. 9. Nondimensional phase speed as a function of wavelength for the Rossby wave ($n = 1$), with vertical shear of $U_T = \pm 5$ m s^{-1} (solid line) and $U_T = 0$ (dashed line). Note the vertical mean zonal flow ($\bar{U}$) vanishes in these calculations in order to identify the influence of vertical shear.

ical computations indicate that the preceding statements are valid for all waves that have a wavelength longer than a few thousands kilometers. Note that in the Tropics between $y = -2$ and $y = 2$ the magnitude of the total baroclinic forcing is similar for both Rossby and Kelvin waves (Figs. 11a and 12a).

Although the baroclinic forcing for the Rossby and Kelvin waves is comparable, the forced barotropic Rossby mode is much stronger than the barotropic Kelvin mode. To find out the cause, let us examine horizontal structures of the fields of barotropic vorticity, barotropic planetary vorticity advection, baroclinic forcing, and barotropic vorticity tendency for Rossby waves (Fig. 11) and Kelvin waves (Fig. 12) in a moderate easterly shear. Notice that the zonal phase of the barotropic planetary vorticity advection is shifted 90° to the west compared to the barotropic vorticity field for both Rossby and Kelvin waves. This is consistent with the phase relationship between the barotropic vorticity ζ_+ and meridional wind v_+. The vorticity tendency associated with the planetary vorticity advection favors the barotropic mode propagating westward. The baroclinic forcing, however, is 180° out of phase with the barotropic planetary vorticity advection for both waves, that is, it is located one-quarter of a wavelength east of the barotropic vorticity field (Figs. 11a and 12a). This implies that the barotropic vorticity tendency generated by the baroclinic forcing promotes an eastward propagation. The total local change of barotropic vorticity must be congruous with the wave's propagation, namely, it is phase-shifted by one-quarter of a wavelength to the west (east) of the barotropic Rossby (Kelvin) mode (Figs. 11d and 12d). In order to maintain the vorticity tendency required by the westward propagation of the Rossby mode, the barotropic planetary vorticity advection must overcome the opposing tendency induced by the baroclinic forcing. That requires a strong v_+, or equivalently, a strong barotropic motion (note that for nondivergent barotropic motion its strength is fully represented by v_+). Conversely, in order to maintain the vorticity tendency required by the eastward propagation of the Kelvin mode, the baroclinic forcing must overcome the barotropic planetary vorticity advection. That puts a strict limit on the magnitude of v_+; thus, the barotropic motion must be sufficiently weak. In summary, the barotropic mode is, in nature, a Rossby-like vorticity wave, its excitation by baroclinic Rossby wave forcing is a resonant response in the sense that the resounding response occurs only when the baroclinic forcing moves in harmony with the propagation of the intrinsic barotropic mode.

It is worthwhile to mention that the baroclinic forcing for the Rossby wave has considerable magnitude in high latitudes, whereas it is confined to the Tropics in the Kelvin wave case (Figs. 11a and 12a). This is because the maximum amplitude for the baroclinic Kelvin mode is at the equator, whereas for baroclinic Rossby waves, it is at one to two Rossby radii of deformation away from the equator (Fig. 6). The difference in the strength of baroclinic forcing in the extratropics may also contribute to the enhancement of high-latitude barotropic response.

5. Effects of meridional variation of the vertical shear

In general, the zonal flow has both meridional and vertical variations. To simplify the problem, consider the following mean flow:

$$U_1 = \bar{U} + U_T(y), \quad U_2 = \bar{U} - U_T(y), \quad (5.1)$$

where $\bar{U}$ is a constant and U_T is a function of y. Here, we have neglected meridional variation of the vertical mean flow but retained meridional variation of the vertical shear. Using a similar approach as used in section 4, one can obtain the following governing equations:

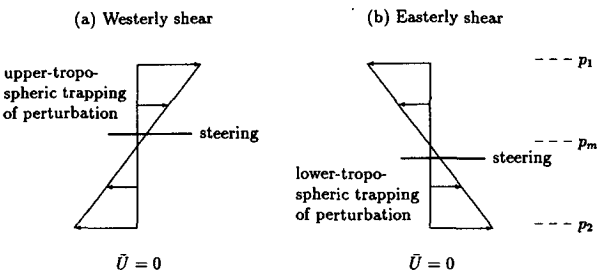

FIG. 10. Schematic diagram displaying steering level in (a) a westerly vertical shear and (b) an easterly vertical shear for Rossby waves.

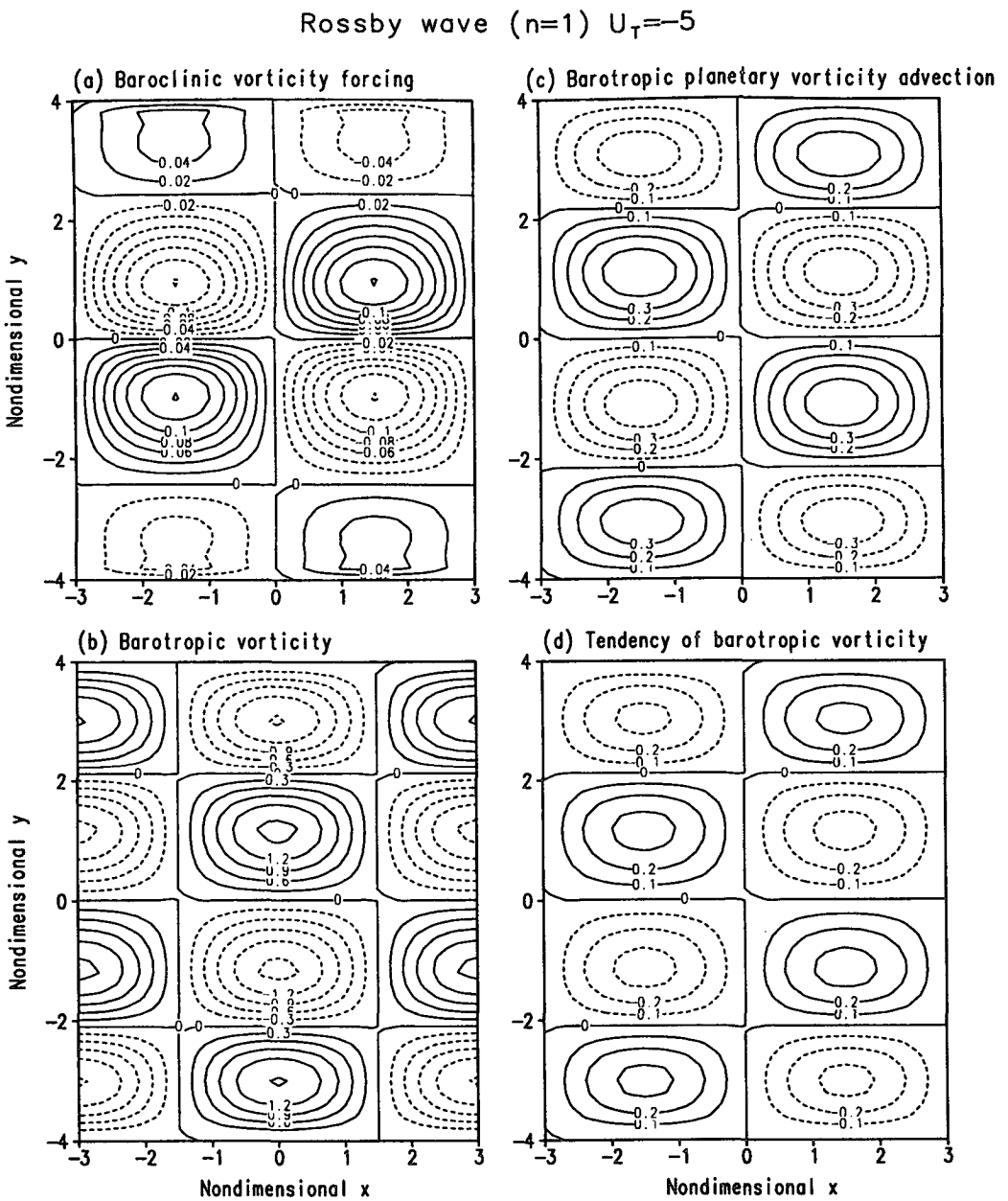

FIG. 11. Horizontal structures of (a) baroclinic forcing, (b) barotropic vorticity, (c) barotropic planetary vorticity advection, and (d) tendency of barotropic vorticity for the Rossby wave (n = 1) with a wavelength of 10 000 km in an easterly vertical shear (U_T = −5 m s^{-1}).

$$\frac{D}{Dt}\nabla^2\psi + \frac{\partial\psi}{\partial x} = U_T\left[\left(\frac{\partial^2}{\partial y^2} - \frac{\partial^2}{\partial x^2}\right)v_- + 2\frac{\partial^2 u_-}{\partial x\partial y}\right] + 2U_T'\left(\frac{\partial u_-}{\partial x} + \frac{\partial v_-}{\partial y}\right) + U_T''v_-, \quad (5.2a)$$

$$\frac{Du_-}{Dt} - yv_- + \frac{\partial\phi_-}{\partial x} = -U_T\frac{\partial u_+}{\partial x} - v_+U_T', \quad (5.2b)$$

$$\frac{Dv_-}{Dt} + yu_- + \frac{\partial\phi_-}{\partial y} = -U_T\frac{\partial v_+}{\partial x}, \quad (5.2c)$$

$$\frac{D\phi_-}{Dt} + \frac{\partial u_-}{\partial x} + \frac{\partial v_-}{\partial y} = yv_+U_T, \quad (5.2d)$$

where ψ is the streamfunction of the barotropic mode and

$$U_T' \equiv \frac{dU_T}{dy}, \quad U_T'' \equiv \frac{d^2U_T}{dy^2}.$$

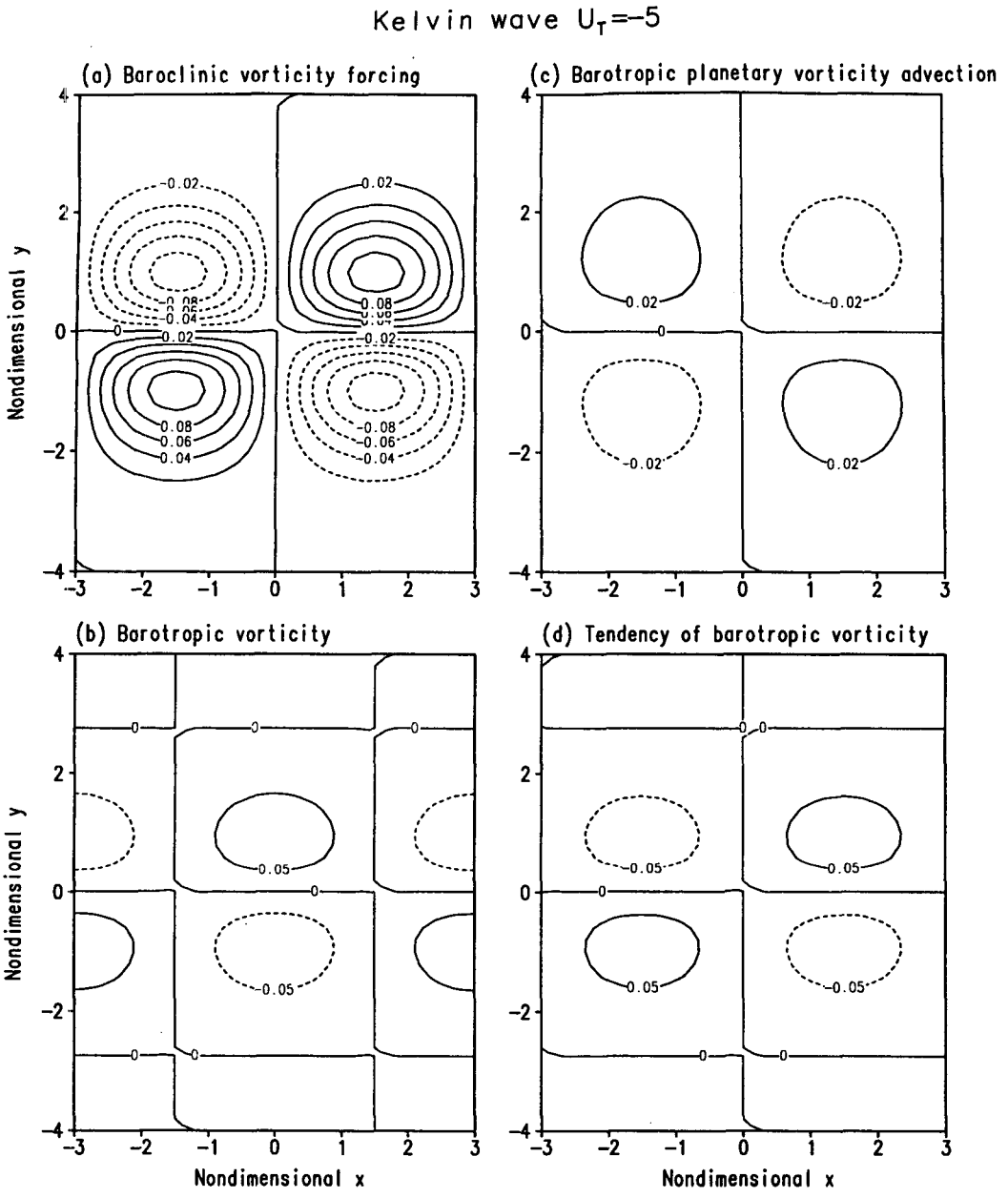

FIG. 12. As in Fig. 11 except for a Kelvin wave.

Using (4.3) in (5.2) and eliminating U and Φ from the resulting equations yields

$$V_{yy} - \left(a^2 + k^2 + y^2 - i\frac{k}{a}\right)V = \frac{k^2}{a}U_T\Psi_{yy} + 2iky U_T\Psi_y + \left[\frac{k^2y^2}{a}U_T + ikU_T - \frac{k^2}{a}U_T'' - \frac{k^2}{a}(a^2 + k^2)U_T\right]\Psi, \quad (5.3a)$$

$$a_1\Psi_{yy} + a_2\Psi_y + a_3\Psi = a_4V_{yy} + a_5V_y + a_6V, \quad (5.3b)$$

where

$$a \equiv ik(\bar{U} - c),$$

$$a_1 = a(a^2 + k^2) + 2ak^2U_T^2,$$

$$a_2 = 2ak^2U_TU_T' - 2ik^3yU_T^2,$$

$$a_3 = -(a^2 + k^2)(k^2a - ik) - 2k^2aU_TU_T'' - 2ik^3U_T^2 - 4ik^3yU_TU_T' - 2ak^2U_T'^2,$$

$$a_4 = (a^2 - k^2)U_T,$$

$$a_5 = 2a^2U_T' + 2ikayU_T,$$

$$a_6 = (a^2 + k^2)(k^2U_T + U_T'') + 2ikaU_T + 2ikayU_T'.$$

Consider two cases in which $\bar{U} = 0$ but U_T are, respectively, symmetric and asymmetric about the equator:

$$U_T = \begin{cases} \text{UTS} = S_1\left(1 - \cos\dfrac{\pi y}{3}\right), \\ \text{UTA} = S_2\left(1 - \cos\dfrac{\pi(y-1)}{3}\right), \end{cases}$$

where $S_1 = 4.1$ m s^{-1} and $S_2 = 4.4$ m s^{-1}. The two vertical shear profiles are displayed in Fig. 13. The meridionally averaged shear in both cases equals 5 m s^{-1}, so that results can be compared with those derived in the constant vertical shear case ($U_T = 5$ m s^{-1}).

Structures of the baroclinic and barotropic Rossby modes in a symmetric shear (U_T = UTS) bear great similarity to those in a constant shear ($U_T = 5$ m s^{-1}), except that the baroclinic mode for the former is slightly weaker between $y = \pm 2$ but stronger poleward (Figs. 14a and 14c). This difference is due primarily to the fact that the vertical shear UTS is smaller near the equator while larger than 5 m s^{-1} poleward of $y = \pm 1.5$. The larger vertical shear in the midlatitudes enhances the baroclinic response in the higher latitudes.

With an asymmetric shear (U_T = UTA), both the baroclinic and barotropic modes exhibit an asymmetry in their meridional structure (Fig. 14b), which results from latitudinal variations of the strength of vertical shear. The shear UTA has maxima near $y = -2$ and $y = 3$. For the baroclinic mode the maximum shears enhance cyclonic (anticyclonic) flows south of the equator and wave perturbation in the northern extratropics. For the barotropic mode, intensified wind and geopotential perturbation is also found when local vertical shear is enhanced. It is concluded that as the vertical shear varies with latitude the shear strength in situ is important to modification of the low-frequency equatorial waves.

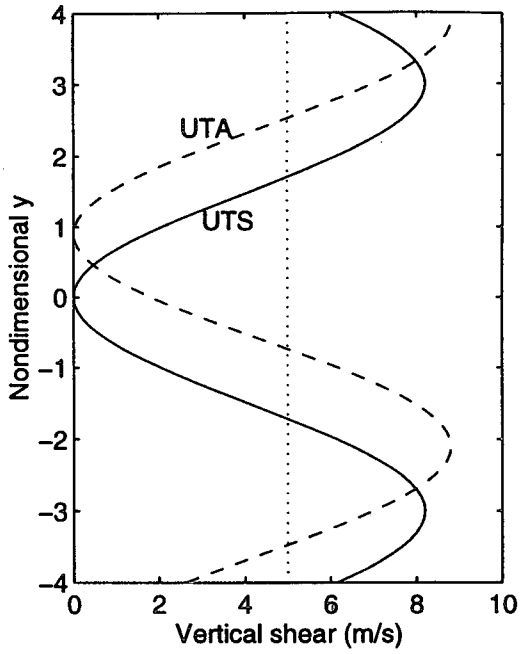

FIG. 13. Profiles of meridionally varying vertical shears with a symmetric (UTS) and an asymmetric (UTA) structure. Latitudinal average of both curves equals 5 m s^{-1}.

6. Conclusions and discussion

a. Conclusions

Effects of a basic zonal flow with vertical and meridional shears on vertically standing, low-frequency equatorial waves (the Kelvin wave, the Rossby wave with a gravest meridional structure, and the westward propagating Yanai wave) are investigated using simple two-level models on an equatorial β plane and spherical coordinates. The simplicity of the β-plane model allows for a better understanding of the mechanism by which basic flows alter wave dynamics.

The vertical shear of a mean zonal flow was found to have profound influences on the equatorial Rossby wave and westward propagating Yanai wave. Meridional shears, however, have only a moderate modification on low-frequency equatorial waves. This is due to the fact that vertical shears couple the baroclinic and barotropic modes; their interaction causes marked changes in wave characteristics, whereas meridional shears do not.

In the presence of a moderate vertical shear, the baroclinic Rossby mode acts to force the barotropic mode. With a westerly (easterly) shear, positive (negative) barotropic vorticity is generated in the region of the longitudinal stretch of baroclinic vorticity. The intensity of the barotropic mode increases with increasing vertical shear. In contrast, with the same shear, a baroclinic Kelvin mode can stimulate only a rather weak barotropic mode. This fundamental difference results from the rotational nature of the barotropic mode, which, in the absence of forcing, is a Rossby wave maintained by an effective β parameter ($\beta - \bar{u}_{yy}$). Because of the intrinsic nature of the barotropic mode, it can only be resonantly excited by a westward propagating baroclinic mode but not by an eastward propagating one.

In the presence of vertical shear, the baroclinic Rossby mode is slightly less equatorially trapped. However, the barotropic Rossby mode extends poleward with zonal wind and geopotential extrema occurring in the extratropics. This implies that a tropical

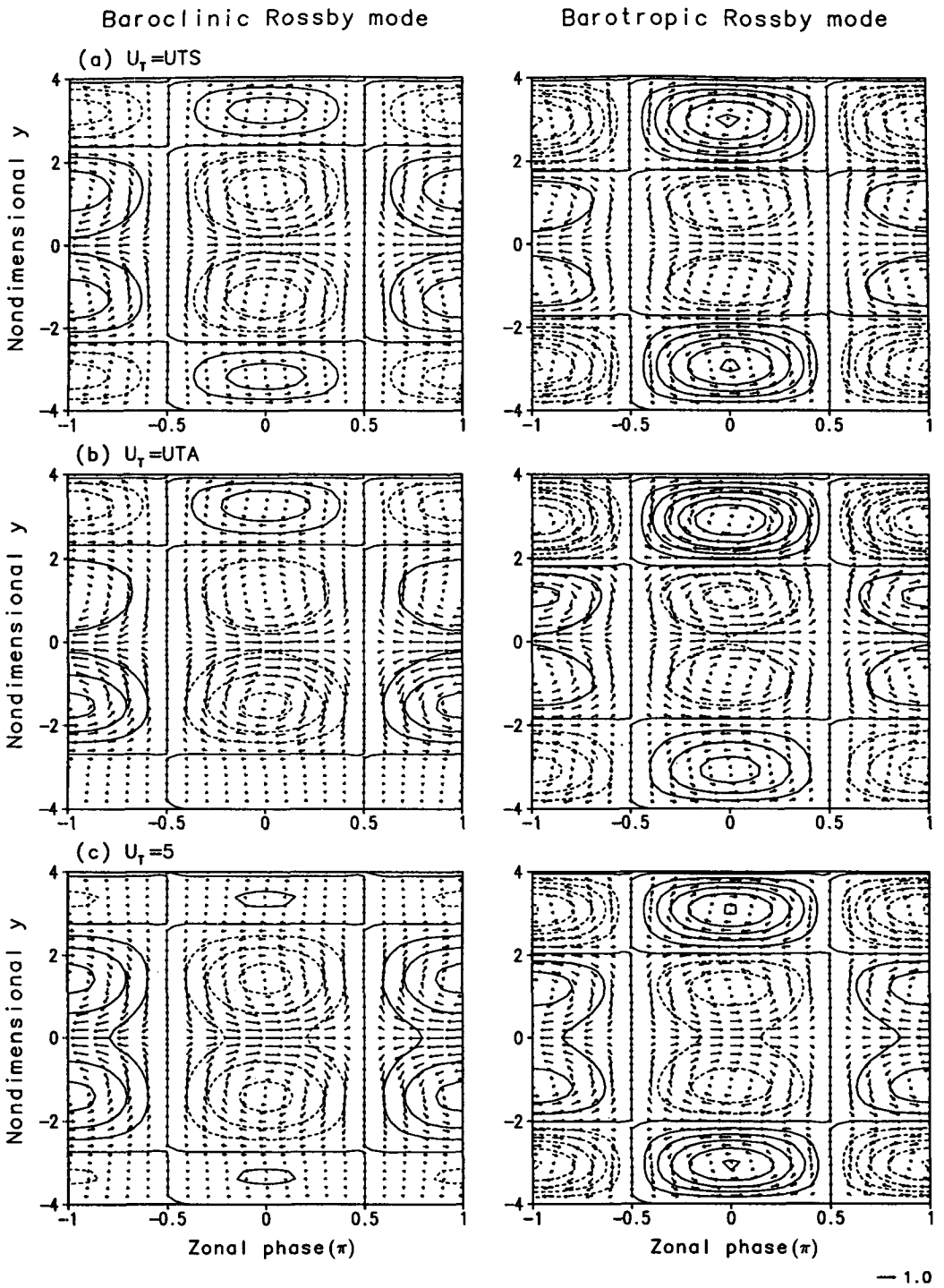

FIG. 14. Geopotential and flow patterns of the baroclinic and barotropic modes for the $n = 1$ Rossby wave with a wavelength of 10 000 km in (a) U_T = UTS, (b) U_T = UTA, and (c) $U_T = 5$ m s^{-1}.

heating-induced internal Rossby mode may generate, with the aid of the vertical shear, a conspicuous barotropic Rossby wave response in the extratropics.

The vertical shear can change vertical modal structure. This is because the coupling of the two vertical modes depends on the sign of the vertical shear. The

barotropic and baroclinic Rossby modes are nearly in phase in a westerly shear (i.e., westerlies increasing with height) whereas they are precisely 180° out of phase in an easterly shear. It follows that the vertical shear creates a vertical asymmetry in the structures of the Rossby wave and westward propagating Yanai waves: the waves in a westerly shear have a larger amplitude in the upper troposphere, whereas the waves in an easterly shear have a greater amplitude in the lower troposphere. This results in a raised (lowered) steering level for the waves in a westerly (easterly) shear. The mean flow steering is thus eastward in both westerly and easterly shears if the vertical mean flow vanishes. The propagation of the Rossby wave is thus slowed down by vertical shear regardless of its sign.

It is shown that both the barotropic and baroclinic Rossby modes respond sensitively to the meridional variation of the vertical shear. The responses are enhanced in the latitudes where the vertical shear is strengthened, suggesting the importance of the regional vertical shear in modification of the in situ wave characteristics.

The vorticity and meridional vorticity gradient associated with a meridional shear can alter the wave refractive index and thus the degree of equatorial trapping for equatorial waves. Longer waves are less affected than shorter waves. Due to the wavelength-dependent modification of the meridional structure and the nonuniform zonal advection by meridionally sheared flows, Kelvin waves become weakly dispersive, and the Rossby waves also experience noticeable changes in their dispersivity.

b. *Discussion*

One of the fundamental impacts of the vertical shear is the excitation of prominent barotropic Rossby wave motion through an interaction with the gravest baroclinic Rossby mode. This is relevant to the explanation of the *emanation* of equatorial waves toward midlatitudes. The energy emanation was suggested as resulting from the reduction of the equatorial trapping scale of the Rossby waves in equatorial westerlies (Zhang and Webster 1989). We have shown that the direction of the mean flow does not affect meridional structure of the internal waves. The meridional shear enhances the trapping of the equatorial Rossby waves and cannot generate a barotropic Rossby wave component. Based on our analysis, we infer that the emanation of equatorial waves is associated with an excitation of the barotropic Rossby mode, which is caused by a combined effect of vertical shear and the zonal stretch of the vorticity associated with baroclinic mode. The baroclinic Rossby mode is presumably stimulated directly by the equatorial internal heating. The meridional variation of divergence and longitudinal variation of vorticity associated with the baroclinic mode acting on the vertical shear of the mean flow represent an excitation mechanism for the barotropic (external) motion. This view of emanation explains how an internal equatorial heating can generate a salient extratropical barotropic response. Although tropical heating may initiate both eastward propagating Kelvin wave and westward propagating Rossby waves on a synoptic scale or longer, the intrinsic rotational nature of the barotropic motion endorses a resonant mode selection; that is, only a westward propagating baroclinic Rossby mode can activate a large-amplitude barotropic motion that extends into the extratropics.

Another fundamental impact of the vertical shear on the equatorial Rossby wave is that a westerly (easterly) vertical shear favors trapping wave kinetic energy to the upper (lower) troposphere. This may be pertinent to interpretation of the *in-phase* relationship between the transient kinetic energy and the equatorial mean zonal flow in the upper troposphere, as observed by Murakami and Unninayer (1977) and Arkin and Webster (1985). Over the regions of upper-level westerlies (easterlies), the mean zonal flow is characterized by westerly (easterly) shear because of the dominance of the upper-tropospheric zonal winds. The vertical structure of the Rossby wave can be so modified by the vertical shear that the wave kinetic energy tends to be confined in the upper-tropospheric westerlies. On the other hand, in a region of upper-level easterlies (easterly shear), the upper-level perturbation kinetic energy may be reduced due to the concentration of the perturbation in the lower troposphere. It is plausible, therefore, that the in-phase relationship between upper-tropospheric perturbation kinetic energy and time-mean zonal flow may be a result of the transformation in vertical modal structure between the regions of easterly and westerly shear along the equator. In order to verify the present theory, it would be interesting to compute transient kinetic energy in the lower troposphere and check whether they have maxima in the easterly shear region and minima in the westerly shear region. It would also be interesting to explore the transition of the vertical structure of equatorial waves from regions of easterly to westerly shear.

The investigation in this paper is confined to neutral waves in a moderate vertical shear. It should be pointed out that strong vertical shears can result in dynamically unstable Rossby waves even in an adiabatic, stably stratified atmosphere. This type of dynamic instability and the effects of sheared flow on diabatic equatorial waves will be reported in Part II.

Acknowledgments. This work has been supported by the Climate Dynamics Program of the National Science Foundation under Grants ATM90-19315 and ATM94-00759. This is the School of Ocean and Earth Science and Technology publication number 3971.

APPENDIX

Governing Equations in Spherical Coordinates

Consider a basic zonal flow that varies with latitude and height and satisfies the gradient wind balance. The governing equations for inviscid, hydrostatic, perturbation motions in spherical pressure (p) coordinates are

$$\frac{\partial u}{\partial t} + \bar{u}\frac{\partial u}{\partial x} + \omega\frac{\partial \bar{u}}{\partial p} - \left(f - \frac{d(\bar{u}\cos\varphi)}{\cos\varphi dy}\right)v = -\frac{\partial \phi}{\partial x}, \tag{A1a}$$

$$\frac{\partial v}{\partial t} + \bar{u}\frac{\partial v}{\partial x} + \left(f + \frac{2\bar{u}\tan\varphi}{a}\right)u = -\frac{\partial \phi}{\partial y}, \tag{A1b}$$

$$\frac{\partial u}{\partial x} + \frac{\partial(v\cos\varphi)}{\cos\varphi\partial y} + \frac{\partial \omega}{\partial p} = 0, \tag{A1c}$$

$$\frac{\partial}{\partial t}\left(\frac{\partial \phi}{\partial p}\right) + \bar{u}\frac{\partial}{\partial x}\left(\frac{\partial \phi}{\partial p}\right) - \left(f + \frac{2\bar{u}\tan\varphi}{a}\right) \times v\frac{\partial \bar{u}}{\partial p} + S\omega = -\frac{RQ'}{C_p p}, \tag{A1d}$$

where a is earth's radius, φ is latitude, f is the Coriolis parameter, and other symbols have the same definition as in Eqs. (2.1a–d).

All dependent variables were split into barotropic and baroclinic modes defined by (2.4), and the governing equations were nondimensionalized using the velocity scale $C_m = (0.5\Delta p^2 S_m)^{1/2}$, horizontal length scale $L = a$, timescale a/C_m, geopotential scale C_m^2, and vertical p-velocity scale $2\Delta p C_m/a$. Introducing a barotropic streamfunction as (4.1), equations analogous to (4.2) for a constant vertical shear in spherical coordinates are

$$\frac{D}{Dt}\nabla^2\psi + \tilde{f}_y\frac{\partial \psi}{\partial x} = U_T\left[\frac{\partial^2(v_-\cos\varphi)}{\cos\varphi\partial y^2} - \frac{\partial^2 v_-}{\partial x^2} - \frac{\partial(v_-\sin\varphi)}{\cos\varphi\partial y}\right] + 2U_T\left(\frac{\partial^2 u_-}{\partial x\partial y} - \tan\varphi\frac{\partial u_-}{\partial x}\right), \tag{A2a}$$

$$\frac{Du_-}{Dt} - \tilde{f}v_- + \frac{\partial \phi_-}{\partial x} = -U_T\frac{\partial u_+}{\partial x} + U_T\tan\varphi v_+, \tag{A2b}$$

$$\frac{Dv_-}{Dt} + \tilde{f}u_- + \frac{\partial \phi_-}{\partial y} = -U_T\frac{\partial v_+}{\partial x} - 2U_T\tan\varphi u_+, \tag{A2c}$$

$$\frac{D\phi_-}{Dt} + \frac{\partial u_-}{\partial x} + \frac{\partial(v_-\cos\varphi)}{\cos\varphi\partial y} = \hat{f}v_+U_T, \tag{A2d}$$

where

$$\tilde{f} = \frac{a}{C_m}2\Omega\sin\varphi + \bar{U}\tan\varphi, \tag{A3a}$$

$$\hat{f} = \frac{a}{C_m}2\Omega\sin\varphi + 2\bar{U}\tan\varphi, \tag{A3b}$$

$$\tilde{f}_y = \frac{a}{C_m}2\Omega\cos\varphi + \bar{U}\sec^2\varphi. \tag{A3c}$$

Seeking wave solutions of the form (4.3) and eliminating Φ and U leads to

$$\left(1 + \frac{2U_T^2}{1-c'^2}\right)\Psi_{yy} - \left[\frac{2\hat{f}U_T^2}{c'(1-c'^2)} + \tan\varphi\right]\Psi_y - \left[k^2 - \frac{\tilde{f}_y}{c'} + \frac{2U_T^2\hat{f}_y}{c'(1-c'^2)} - \frac{2U_T^2}{1-c'^2}\left(1 + \frac{\hat{f}\tan\varphi}{c'}\right)\right]\Psi = \frac{iU_T}{kc'}\left[\frac{1+c'^2}{1-c'^2}V_{yy} + \frac{2c'\tilde{f} - (1+3c'^2)\tan\varphi)}{1-c'^2}V_y - \left(k^2 - \frac{2c'\tilde{f}_y - 2c'\hat{f}\tan\varphi - 2c'^2}{1-c'^2}\right)V\right], \tag{A4a}$$

$$V_{yy} - \left(1 + \frac{\bar{U}}{c'}\right)\tan\varphi V_y - \left[\tilde{f}\hat{f} + k^2(1-c'^2) - \frac{\tilde{f}_y}{c'} - \frac{\hat{f}\tan\varphi}{c'} + \sec^2\varphi\right]V = -\frac{ikU_T}{c'} \times [\Psi_{yy} - (2\hat{f}c' + (1-2c'^2)\tan\varphi)\Psi_y - (k^2(1-c'^2) + c'(\hat{f}_y + \hat{f}\tan\varphi) - \hat{f}^2 - \sec^2\varphi)\Psi], \tag{A4b}$$

where $c' = \bar{U} - c$,

$$\hat{f}_y = \frac{a}{C_m}2\Omega\cos\varphi + 2\bar{U}\sec^2\varphi.$$

REFERENCES

Arkin, P., and P. J. Webster, 1985: Annual and interannual variability of the tropical–extratropical interaction: An empirical study. *Mon. Wea. Rev.*, **113**, 1510–1523.

Boyd, J. P., 1978a: The effects of latitudinal shear on equatorial waves. Part I: Theory and methods. *J. Atmos. Sci.*, **35**, 2236–2258.

——, 1978b: The effects of latitudinal shear on equatorial waves. Part II: Applications to the atmosphere. *J. Atmos. Sci.*, **35**, 2259–2267.

Charney, J. G., 1969: A further note on the large scale motions in the tropics. *J. Atmos. Sci.,* **26,** 182–185.

Holton, J. R., 1970: The influence of mean wind shear on the propagation of Kelvin waves. *Tellus,* **22,** 186–193.

Horel, J. D., and J. M. Wallace, 1981: Planetary-scale atmospheric phenomena associated with the Southern Oscillation. *Mon. Wea. Rev.,* **109,** 813–829.

Hoskins, B. J., and D. Karoly, 1981: The steady linear response of a spherical atmospheric to thermal and orographic forcing. *J. Atmos. Sci.,* **38,** 1179–1196.

——, and F. Jin, 1991: The initial value problem for tropical perturbations to a baroclinic atmosphere. *Quart. J. Roy. Meteor. Soc.,* **117,** 299–317.

Kasahara, A., and P. L. Silva Dias, 1986: Response of planetary waves to stationary tropical heating in a global atmosphere with meridional and vertical shear. *J. Atmos. Sci.,* **43,** 1893–1911.

Langer, R. E., 1960: *Boundary Problems in Differential Equations.* University of Wisconsin Press, 243–255.

Lau, K.-M., and H. Lim, 1984: On the dynamics of equatorial forcing of climate teleconnections. *J. Atmos. Sci.,* **41,** 166–176.

Lim, H., and C.-P. Chang, 1983: Dynamics of teleconnections and Walker circulations forced by equatorial heating. *J. Atmos. Sci.,* **40,** 1897–1915.

——, and ——, 1986: Generation of internal- and external-mode motions from internal heating: Effects of vertical shear and damping. *J. Atmos. Sci.,* **43,** 948–957.

Lindzen, R. S., 1970: Internal equatorial planetary-scale waves in shear flow. *J. Atmos. Sci.,* **27,** 394–407.

Matsuno, T., 1966: Quasi-geostrophic motions in the equatorial area. *J. Meteor. Soc. Japan,* **44,** 25–43.

Murakami, T., and S. Unninayer, 1977: Atmospheric circulation during December 1970 through February 1971. *Mon. Wea. Rev.,* **105,** 1024–1038.

——, and B. Wang, 1993: Annual cycle of equatorial east–west circulation over the Indian and Pacific Oceans. *J. Climate,* **6,** 932–952.

Wang, B., and H. Rui, 1990: Dynamics of the coupled moist Kelvin–Rossby wave on an equatorial β-plane. *J. Atmos. Sci.,* **47,** 397–413.

Wallace, J. M., and D. S. Gutzler, 1981: Teleconnections in the geopotential height field during the Northern Hemisphere winter. *Mon. Wea. Rev.,* **109,** 784–812.

Webster, P. J., 1972: Response of the tropical atmosphere to local steady forcing. *Mon. Wea. Rev.,* **100,** 518–541.

——, 1981: Mechanisms determining the atmospheric response to sea surface temperature anomalies. *J. Atmos. Sci.,* **38,** 554–571.

——, and J. R. Holton, 1982: Cross equatorial response to midlatitude forcing in a zonally varying basic state. *J. Atmos. Sci.,* **39,** 722–733.

——, and H. R. Chang, 1988: Equatorial energy accumulation and emanation regions: Impacts of a zonally varying basic state. *J. Atmos. Sci.,* **45,** 803–829.

Wilson, J. D., and M. K. Mak, 1984: Tropical response to lateral forcing with a latitudinally and zonally nonuniform basic state. *J. Atmos. Sci.,* **41,** 1187–1201.

Yanai, M., and T. Mauryama, 1966: Stratospheric wave disturbance propagating over the equatorial Pacific. *J. Meteor. Soc. Japan,* **44,** 291–294.

Zhang, C., and P. J. Webster, 1989: Effects of zonal flows on equatorially trapped waves. *J. Atmos. Sci.,* **46,** 3632–3652.